Environ Sci Pollut Res (2016) 23:8917–8928
DOI 10.1007/s11356-016-6125-3

RESEARCH ARTICLE

Classification of diurnal patterns of particulate inorganic ions downwind of metropolitan Seoul

Yong Hwan Lee[1,2] · **Yongjoo Choi**[1] · **Young Sung Ghim**[1]

Received: 23 October 2015 / Accepted: 18 January 2016 / Published online: 28 January 2016

Abstract The inorganic ions in $PM_{2.5}$ were measured downwind of metropolitan Seoul using a particle-into-liquid sampler over three periods. Five diurnal patterns, including a low-concentration pattern (L) and a high-concentration pattern with a decreasing trend during the day (H-), were distinguished for the first period from February to June 2012. The sum of ion concentrations increased primarily due to NO_3^- with decreasing temperature and increasing relative humidity, which caused preferential partitioning of NO_3^- into the particulate phase. The peak concentration occurred during the morning rush hour for L but was delayed until the next morning for H- due to the time required to form secondary inorganic ions from accumulated pollutants under lower wind speeds. The characteristic features of the patterns observed during the first period were generally similar with those obtained for the other two periods. However, for the second period, comprised of colder months, changes in the diurnal patterns from L to H- were accompanied by increasing temperature, as the effect of photochemical formation of NO_3^- was larger than that of volatilization. Although the role of long-range transport was not distinct on the whole, the inflow of air masses from cleaner sectors was observed to lower the concentrations.

Keywords Particle-into-liquid sampler · Cluster analysis · Nitrate · Peak time · Secondary formation

Responsible editor: Gerhard Lammel

✉ Young Sung Ghim
ysghim@hufs.ac.kr

[1] Department of Environmental Science, Hankuk University of Foreign Studies, Yongin 17035, South Korea

[2] Present address: Department of Air Quality Research, National Institute of Environmental Research, Incheon 22689, South Korea

Introduction

Fine particles are not only hazardous to human health but also are crucial to visibility and climate change due to effective scattering and absorption of solar radiation (Watson, 2002; WHO, 2006; IPCC, 2013). Inorganic ions are major components of fine particles, along with carbonaceous materials and trace elements. The inorganic ions in particles have traditionally been measured using filter sampling followed by ion chromatography (IC) analysis. However, this type of measurement is basically manual, requires much labor, and is prone to errors during various works with filters (Chow, 1995). Nevertheless, the results from filter measurements provide a reference for those from newly developed methods, since the chemical composition of particles has mostly been measured using such techniques (Solomon and Sioutas, 2008; Wittig et al., 2004).

During the past two decades, many continuous and semi-continuous methods for measuring particle composition have been developed (Chow et al., 2008; Solomon et al., 2008). Among them, semi-continuous methods in which particles are solubilized and analyzed with IC have advantages over the other semi-continuous methods such as Stolzenburg and Hering (2000) and Fine et al. (2003) in that they can provide highly time-resolved data by altering the sampling process of the filter-based method. The early types developed by Simon and Desgupta (1995) and Khlystov et al. (1995) were commercialized to the particle-into-liquid sampler (PILS, Applikon Analytical), the monitor for aerosols and gasses in ambient air (MARGA, Applikon Analytical) and the ambient ion monitor (AIM, URG) systems (Makkonen et al., 2012; Thompson et al., 2012; Pancras et al., 2013).

Temporal variation of pollutants results from a series of atmospheric processes such as emission, transport, transformation, and deposition associated with meteorology. Diurnal

and annual variations could be typified by the repetition of meteorology. However, annual variations largely differ depending on the climate and location of the study region. Diurnal variations also differ by region, but the variations caused by activities during the day and night are generally similar. Therefore, the differences from the general patterns of diurnal variation are useful for distinguishing the characteristics of the target area. Nevertheless, there have been limited studies on diurnal variation, particularly for inorganic ions. This is because their concentrations have traditionally been measured using filter sampling, which typically provides daily averages, while highly time-resolved measurements within a day are prerequisite for such studies (Wittig et al., 2004; Millstein et al., 2008).

In the present study, the inorganic ions in $PM_{2.5}$ were measured at a site (127.27°E, 37.34°N, 167 m asl; see Fig. 1 for the location) downwind of Seoul using PILS coupled with IC between the middle of February and early June in 2012. They were also measured for two additional periods until July 2013. In this study, the results from PILS sampling were first compared with those obtained from filter sampling, and the diurnal variations between high- and low-concentration days were examined. Next, diurnal patterns of particulate ions were distinguished using cluster analysis with the data from the first period, and their characteristics were analyzed to find the important features of diurnal variations. Finally, the data during the additional two periods were classified into the patterns obtained for the first period, and the differences in the patterns among the three periods were investigated to ascertain the generality of the patterns identified in this study.

Methods

Measurement site

The measurement was made on the rooftop of a 5-story building located on a hill, about 35 km southeast of downtown Seoul, the general area of which was affected by prevailing northwesterlies. As shown in Fig. 1, the site was in a valley sloping up to the east; the west side was a rural area with small-sized buildings, farmlands, and open spaces scattered on the sides of a 4-lane road and river. The site was considered to be ideal for exploring the transport of air pollutants and secondary formation by photochemical reactions since there were no major sources of emission nearby except the 4-lane road.

Within the same campus, a monitoring station for studying the pollution characteristics downwind of Seoul was operated for two years from March 2008 (Seoul Institute, 2010; Choi

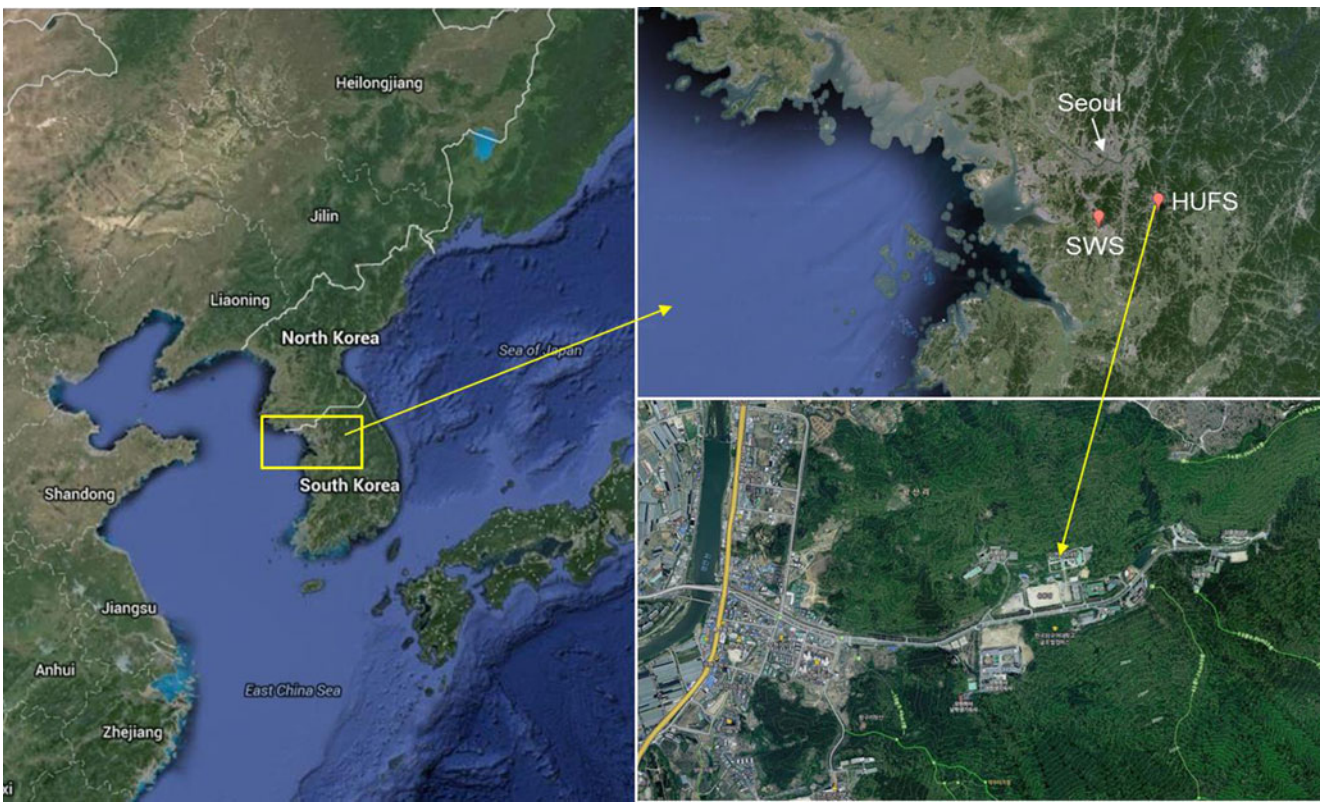

Fig. 1 Location of the measurement site at the Global Campus of Hankuk University of Foreign Studies (HUFS). The Suwon Weather Station (SWS) in the upper-right panel is located about 26 km southwest of HUFS. The 4-lane national road, located 1.4 km to the west of the measurement site, is shown as an *orange line* on the left-hand side of the lower-right panel

et al., 2014). The concentrations of NO and CO, mostly emitted from vehicles, were similarly low to those from a background station, while the ozone concentration was higher compared with other stations within Seoul. The concentration of total suspended particles (TSP) was also higher due to the effect of fugitive dust, which is generally significant in rural areas in Korea. In the measurements of PM_{10} conducted in spring and fall of both 2007 and 2008 at the same site, K^+ was highly correlated with secondary inorganic ions such as SO_4^{2-} and NO_3^-, indicating the influence of biomass burning on the photochemical production (Maxwell-Meyer et al., 2004; Ryu et al., 2004, 2007; Won et al., 2010).

Measurement methods

The inorganic ions present in $PM_{2.5}$ were measured using PILS (ADI 2081, Applikon Analytical) coupled with two IC systems (Advanced modules, Metrohm). In the front of PILS, a $PM_{2.5}$ cyclone (URG-2000-30EH) and two annular denuders (URG-2000-30x242-3CSS) coated with Na_2CO_3 and phosphorous acid to remove the acidic and basic gases, respectively, were placed. The air flow rate was 13.5 L/min. It was known that the cut-off diameter of the cyclone increased to around 2.9 μm with decreasing the flow rate from the originally specified rate of 16.7 L/min (http://www.urgcorp.com/index.php/products/inlets/teflon-coated-aluminum-cyclones/33-configurations/153-urg-2000-30eh). However, PILS was operated at this rate because the rate was the most stable, and the difference in $PM_{2.5}$ concentration did not appear to be significant.

Within PILS, the particles in the sampled air were mixed with supersaturated steam, causing them to grow and solubilized to form water droplets (Orsini et al., 2003; Weber et al., 2001, 2003). The droplets were hit onto the impaction surface and subsequently collected by the transport liquid, flowing at a rate of 36.5 μL/min. LiBr of 0.11 μeq/L was added to the transport liquid as an internal standard. The concentration in ambient air was determined by calculating the dilution of the internal standard by the droplets (Orsini et al., 2003).

Three anions (Cl^-, NO_3^-, and SO_4^{2-}) and five cations (Na^+, NH_4^+, K^+, Mg^{2+}, and Ca^{2+}) were analyzed by online ICs. For simultaneous analysis of anions and cations, each sample was loaded into a 250-μL loop and injected into the IC, which took around 25.5 min. Since IC analyses required less time, ions were measured at this time interval. Anions were analyzed using a Metrosep A Supp 5-150/4.0 column with a solution of 3.2 mM Na_2CO_3 and 1.0 mM $NaHCO_3$ as the eluent, and cations were analyzed using a Metrosep C4-150/4.0 column with a solution of 4.0 mM nitric acid as the eluent. The detection limits in $\mu g/m^3$ (uncertainty in %) were 0.021 (2.3) for Cl^-, 0.156 (12.9) for NO_3^-, 0.034 (7.4) for SO_4^{2-}, 0.014 (6.3) for Na^+, 0.010 (3.1) for NH_4^+, 0.008 (34.1) for K^+, 0.006 (12.9) for Mg^{2+}, and 0.012 (16.5) for Ca^{2+}. Both values were determined by analyzing standard solutions of minimum concentrations, which were used for the IC calibration, six times referring to Lee (2002). Denuders were exchanged around every 2 weeks. IC calibration was checked using a medium-range concentration when eluent bottles were filled every 3 or 4 days.

For comparison with the measurement results from PILS sampling, $PM_{2.5}$ was also sampled using a low-volume air sampler consisting of denuders, a Teflon filter, and a backup filter and denuder. Sampling was carried out for 24 hours, from around 10 o'clock in the morning, at a flow rate of 16.7 L/min. The $PM_{2.5}$ inlet and upstream denuders were the same as those of the PILS system. A two-stage filter pack (URG-2000-22FB) had a Teflon filter (Zefluor, Pall) to collect fine particles and a backup Nylon filter (Nylasorb, Pall) to collect acid gases produced from fine particles. The backup denuder was coated with phosphorous acid to collect basic gases from fine particles.

After sampling, the Teflon filters were immersed in a mixture of 1 mL ethanol and 14 mL deionized water and sonicated to dissolve the water-soluble ions. Nylon filters were extracted similarly, but using the eluent for anion analysis. The denuders were extracted using 10 mL deionized water. IC analysis of the extracts was carried out in the same way as for the PILS liquid samples. The detection limits of IC for filter samples, which used a 20-μl sample loop, in $\mu g/m^3$ (uncertainties in %) were 0.040 (4.9) for Cl^-, 0.058 (4.2) for NO_3^-, 0.057 (3.3) for SO_4^{2-}, 0.062 (21.4) for Na^+, 0.010 (15.5) for NH_4^+, 0.010 (8.8) for K^+, 0.007 (10.8) for Mg^{2+}, and 0.045 (7.4) for Ca^{2+}, determined by seven blank samples (Kim et al., 2015). The 24-h averages of the PILS ion concentrations were compared with the sums of the concentrations from the Teflon filters, backup denuders, and Nylon filters.

Meteorological parameters were measured by an automatic weather station (Useem Instruments) at 10-min intervals. However, because the measurements were incomplete, the data from the Suwon Weather Station (SWS; 37.27 °N, 126.98 °E, 34.5 m asl; see Fig. 1 for the location), about 26 km to the west-southwest, were used instead, whose correlation with the on-site data from the automatic weather station was the highest among those from nearby weather stations.

Data analysis

PILS sampling was performed for three periods—the first being between February and June 2012, the second between November 2012 and January 2013, and the third between March and July 2013 (Table 1). If PILS had been fully operated on all sampling days without pause, the total possible number of data for the three periods would have been around 13,158, assuming sampling was carried out at an interval of 25.5 min. A total of 11,837 data were actually obtained,

Table 1 Mean ion concentrations and meteorological parameters by period

Period	Number of the valid days[a]	Concentration (μg/m^3)									WS (m/s)	Temp (°C)	RH (%)
		Sum	Cl^-	NO_3^-	SO_4^{2-}	Na^+	NH_4^+	K^+	Mg^{2+}	Ca^{2+}			
2012.2–6	94	22.89	0.75	8.23	7.64	0.25	5.50	0.27	0.06	0.18	2.03	11.24	64.31
2012.11–2013.1	37	24.86	1.07	8.82	8.39	0.12	6.09	0.36	0.09	0.16	1.46	−0.55	71.97
2013.3–7	43	31.14	1.06	10.59	10.91	0.20	7.84	0.27	0.06	0.21	1.86	9.31	65.87

[a] Number of days giving valid diurnal data. Refer to the text for the meaning of valid diurnal data

indicating the rate of operation of 90 %. The ion balance of the data was checked using the relative ion difference, the Global Atmospheric Watch (GAW) criteria suggested by Allan (2004). This resulted in the valid data of 10,717, constituting 91 % of the total data. The possible number of data from the full operation of PILS during one day is 56.5, that is, between 56 and 57. The diurnal data were regarded as valid for investigating the diurnal patterns when at least 75 % of the possible data for a day (i.e., 43 out of 56.5) were available. A total of 9324 data for 174 days during the three periods were analyzed, as shown in Table 1, which had an average of 53.6 data per day (95 % of the 56.5).

The numbers of days for which diurnal data were valid (hereafter referred to as the valid days) accounted for 86, 52, and 35 % of the total number of days for the first, second, and third periods, respectively. Differences among the periods were caused by the fact that sampling during the first period was continuous, excluding pauses for instrument maintenance, while that during the other periods was intermittent. Because the sampling was generally started on polluted days rather than cleaner days, the sum of ion concentrations was the highest for the third period, whose number of sampling days (as well as that of the valid days) comprised the smallest fraction of the total number of days. Since the second and third periods were included for assessment of the generality of the patterns identified for the first period, they were divided so that each period could have a reasonable number of the valid days.

Although the number of data on the valid days was sufficiently large, the sampling times varied from day to day because of the sampling interval of 25.5 min. Therefore, the data were resampled at an interval of 30 min using a cubic spline method. The diurnal patterns were distinguished using the data from the first period by an R function, hierarchical clustering (hclust; https://stat.ethz.ch/R-manual/R-devel/library/stats/html/hclust.html) included in the standard R package, "stats" with the option of ward (ward.D in R versions newer than 3.0.3). Another R function, linear discriminant analysis (lda; http://stat.ethz.ch/R-manual/R-patched/library/MASS/html/lda.html), which is provided as a function of the "mass" package, was used to classify the data from the second and third periods into the diurnal patterns identified for the first period.

Separation of the diurnal patterns with increasing number of clusters is shown in Fig. 2. The first three clusters represented low, medium, and high concentrations. Upon increase of the number of clusters to four, the high-concentration cluster was divided into two clusters in which the concentrations were increasing and decreasing during the day. With increase of the number of clusters to five, the medium-concentration cluster was also divided into two clusters, whose primary peaks occurred in the morning and in the afternoon each. At six clusters, further division of the high-concentration cluster with an increasing trend was observed, resulting in two groups whose rates of increase were rapid and moderate. The last division appeared to be relatively insignificant, so five was chosen as the optimum number of clusters.

Results and discussion

Comparison of ion concentrations between PILS and filter measurements

Comparison of ion concentrations determined from PILS sampling with those obtained from filter sampling is shown in Fig. 3. A total of 135 data for which both PILS and filter sampling were available were compared. They accounted for 78 % of the total number of the valid days (174) shown in Table 1. In the case of the sum of ion concentrations, the slope of the best fit line (the slope, hereafter) was 0.83, and the coefficient of the determinant (R^2) was 0.84. Since the intercept was close to zero, the ion sum of PILS concentration was around 83 % of that of the filter concentration on average. R^2 values for ions of higher concentrations, such as secondarily formed SO_4^{2-}, NO_3^-, and NH_4^+, were relatively high between 0.73 and 0.86, while those for ions of lower concentrations, such as Ca^{2+} and Mg^{2+}, were lower at 0.34 and 0.27, respectively (note that the relationships for NH_4^+ and Mg^{2+} are not shown). Similar to the R^2 values, the slopes for secondary ions were between 0.74 and 0.81, while those for Ca^{2+} and Mg^{2+} were lower at 0.49 and 0.30, respectively. R^2 and the slope for

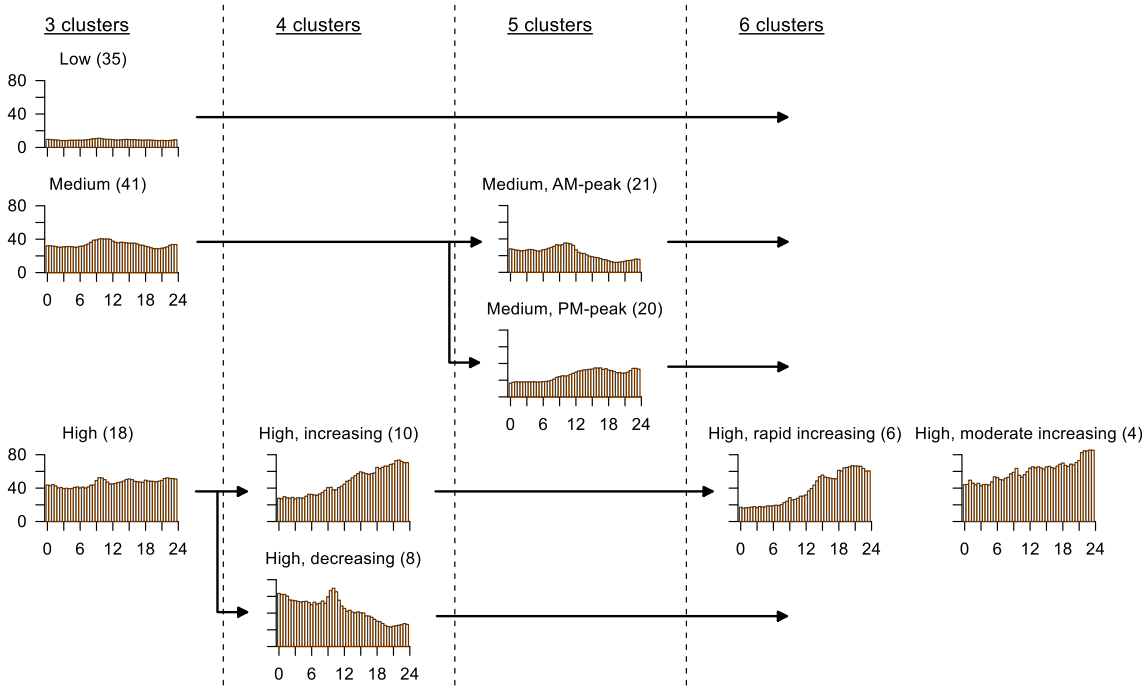

Fig. 2 Separation of diurnal patterns with increasing the number of clusters for the first period. Each *plot* shows the sum of particulate ion concentrations in μg/m^3 vs. hour of the day. *Numbers in the parentheses* indicate the number of days

K^+ were 0.51 and 0.61, respectively, which were higher than those for Ca^{2+} and Mg^{2+}, despite similar concentrations.

Several studies have compared the results from filter and PILS sampling during the past several years. Lee et al. (2008) compared the results from PILS sampling with those from a filter system similar to that used in the present study, for rural areas including National Parks in the United States. For NH_4^+, SO_4^{2-}, and NO_3^-, the slopes through the origin were from 0.92 to 1.02, and the R^2 values ranged from 0.92 to 0.98. Among the three ions, the values for NH_4^+ were the lowest, due to low concentrations approaching the detection limit at some locations and volatilization during PILS sampling. In the measurements of Malm et al. (2005) at Yosemite National Park, the correlation coefficient (R) for K^+ was high at 0.90, along with SO_4^{2-} and NO_3^-, but those for Cl^- and Ca^{2+}, which were present in low concentrations, were negative. Makonnen et al. (2012) compared the results from MARGA and filter sampling at a Finnish urban site. The slopes and R^2 values of NH_4^+, SO_4^{2-}, and NO_3^- were fairly high, from 0.85 to 0.91 and 0.83 to 0.98, respectively. However, K^+ had a negative slope because a number of the concentrations fell below the detection limit, while those of Ca^{2+} and Mg^{2+} were greater than 3 due to contamination of the sample loop.

With reference to such studies, it can be understood that the R^2 values and slopes obtained in this study fell within relatively reasonable ranges because each ion concentration was well above its detection limit. The ratios of mean concentration to the detection limit were 16.1 and 11.6 for Ca^{2+} and Mg^{2+}, respectively, while they were 228, 58.3, and 35.0 for SO_4^{2-}, NO_3^-, and K^+. Therefore, lower values of R^2 for Ca^{2+} and Mg^{2+} were attributable to their lower concentrations in comparison with their detection limits. The slopes were lower than 1.0 because the collection efficiency of PILS was less than 100 %. Although the collection efficiency mainly depends on particle diameter, it is also affected by the volatilization of semi-volatile species such as NH_4^+ due to high temperature and the acidity of droplets activated by supersaturated steam (Sorooshian et al., 2006). In this study, the slope of NH_4^+ was 0.74, lower than those of SO_4^{2-} and NO_3^- shown in Fig. 3. Lower slopes of Ca^{2+} and Mg^{2+} were presumed to be caused by lower solubilities than those of secondary ions (Orsini et al., 2003).

Comparison of diurnal variations between high- and low-concentration days

Prior to investigating the characteristics of the diurnal patterns determined by cluster analysis, the mean diurnal variations were compared between days of high and low concentrations during the first period, as shown in Fig. 4. Here, the high-concentration (HC) days were defined as those in which the sum of the 24-h average ion concentrations (the sum, hereafter) was in the highest 10 %, above 46.2 μg/m^3, while the low-concentration (LC) days represent those in the lowest 10 %, below 7.5 μg/m^3. On both HC and LC days, the sum showed a peak in the morning. However, the peak on HC days occurred at 09:30 (average between 09:00 and 09:30), which was one hour later than the 08:30 observed on LC days.

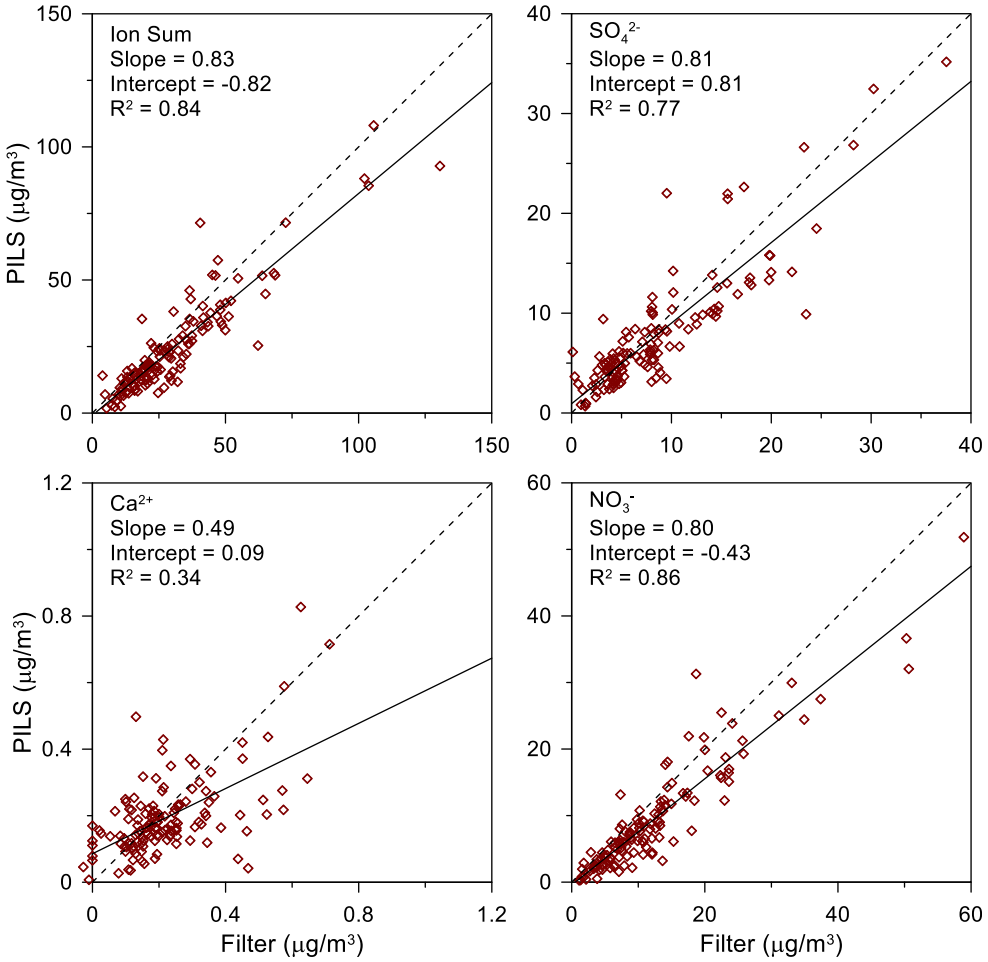

Fig. 3 Comparison of 24-h average concentrations of ions from the PILS sampling with those determined by filter and denuder sampling

In Korea, pollutant concentrations in urban areas increase in the morning due to vehicle emissions during the morning rush hour, with the mixing height still being shallow. After rush hour, the traffic volume does not vary much until late night, but the concentrations due to vehicle emissions decrease with increasing mixing height in the afternoon and increase again at night with decrease of the mixing height. Examination of the variation in the mean concentrations from 14 stations in Seoul between 2002 and 2008 showed that 1-h average peak concentrations occurred in the morning at 09:00 for CO, 10:00 for NO_2, and 11:00 for $PM_{2.5}$ on high $PM_{2.5}$ days (Ghim et al., 2015). Since NO_2 is not only directly emitted but also produced from photochemical reactions, it can reasonably be postulated that the occurrence of the $PM_{2.5}$ peak one hour later than the NO_2 peak, as well as the NO_2 peak one hour later than the CO peak, was due to the time required for the photochemical production of secondary NO_2 and particles (Fujita et al., 2003; Edgerton et al., 2006; Fine et al., 2008).

The statistics of the ions and meteorological parameters on HC and LC days are provided in Table 2. In the lower part of the table, it can be seen that the fraction of SO_4^{2-} was the highest on LC days, while that of NO_3^- was the highest on HC days. The fraction of secondary ions including NH_4^+, SO_4^{2-}, and NO_3^- increased from 89 % on LC days to 96 % on HC days, primarily due to NO_3^-. Millstein et al. (2008) observed peak NO_3^- between 8 a.m. and noon at four sites in the United States, which occurred earlier in the day in spring and summer compared to fall and winter. They explained that this result was because of a combination of factors, including ammonium nitrate dissociation and the onset of convective mixing that occurs earlier in the day in spring and summer. In Fig. 4, peak NO_3^- on HC days also occurred at 09:30, along with the sum of ion concentrations. This earlier occurrence of the peak NO_3^- was probably because the measurements were made in spring.

The wind speed and temperature on HC days were lower than those on LC days, as shown in Table 2. Considering that the NO_3^- concentration was particularly high on HC days, it can be interpreted that the pollutants accumulated due to the low wind speeds, and secondarily formed semi-volatile NO_3^- was preferentially partitioned into the particulate phase under the favorable conditions of low temperature (Seinfeld and Pandis, 1998). However, the difference in relative humidity (RH) was not distinct.

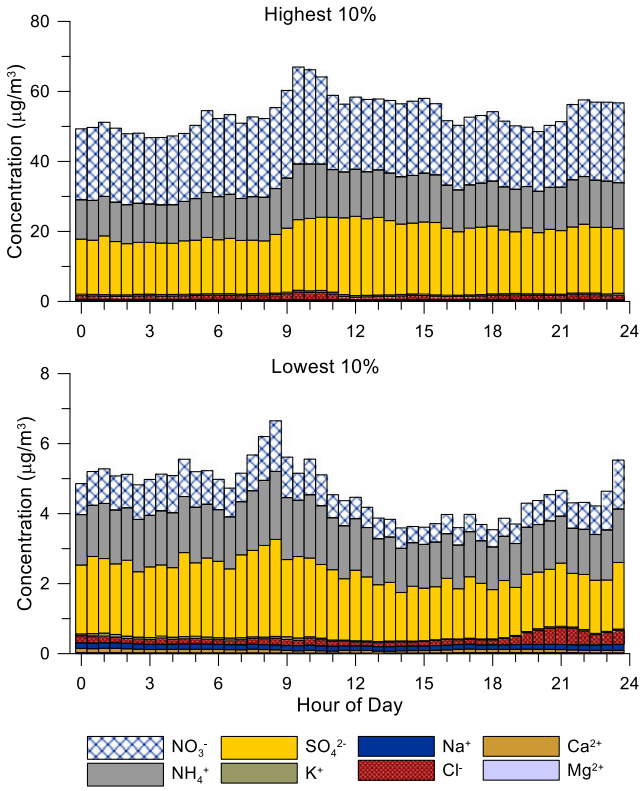

Fig. 4 Mean diurnal variations of ion concentrations on high- and low-concentration days when the sums of the 24-h average ion concentrations were in the highest and lowest 10 %, respectively, for the first period

Characteristics of diurnal patterns

The five patterns of diurnal variations determined by cluster analysis are shown in Fig. 2. The one low-concentration (L) pattern, two medium-concentration patterns (M) with primary morning (am) and afternoon (pm) peaks, and two high-concentration patterns (H) with increasing (+) and decreasing (−) trends during the day were denoted in the figure as L, Mam, Mpm, H+, and H-, respectively. Figure 5 shows the occurrences of the five patterns for the first period. L patterns were located around the line indicating the lowest 10 %. In contrast, H+ and H- were in the higher part during increase and decrease, respectively, or at the peak. Mpm was also found at the peak (particularly at the end of the period) or adjacent to H+ and H-, since the mean level of Mpm was higher than that of Mam and its pattern resembled that of H+.

Similarly to Table 2, the data for the five patterns are summarized in Table 3. In the previous section, it was mentioned that the peak in the morning on HC days occurred one hour later than that on LC days. It can be seen in Fig. 5 that the variation on HC days displayed in Fig. 4 resulted from a combination of those of the five H+ and four H- patterns located above the highest 10 % line. This denotes that the variations in Fig. 4 represent the mean characteristic of averaged ones under a given condition.

In Table 3, it is apparent that the peak was delayed with increase of the sum, excluding H-. It was indicated earlier that the pollutant concentrations due to vehicle emissions decreased with mixing height after the morning rush hour while the traffic volume remained at a similar level. If the pollutants sufficiently accumulate due to low wind speeds, the effect of secondary formation could overwhelm that of increase in the mixing height. The more pollutants accumulate, the more secondary ions are produced, which may cause delay in the peak of the sum due to the time required for the formation of secondary ions.

If the peak time of H- in the morning is regarded as that on the next day, the peak time shown in Table 3 steadily fell behind from L to H- with increasing NO_3^- concentration and fraction. The sum also increased from L to H+, but decreased at H- since the concentrations of other ions except NO_3^- had already decreased. Except for NO_3^- and H-, the concentrations of ions generally increased, but their fractions decreased with increase of the sum. Thanks to this, the role of NO_3^- in the increase of the sum became pronounced. This phenomenon was accompanied by low wind speeds, low

Table 2 Statistical summary of high- and low- concentration days[a]

	Number of days	Peak time[b]	Concentration (μg/m³)								
			Sum	Cl^-	NO_3^-	SO_4^{2-}	Na^+	NH_4^+	K^+	Mg^{2+}	Ca^{2+}
HC	9	9:30	53.9 ± 7.5	1.23 ± 0.51	20.9 ± 0.8	18.1 ± 5.2	0.29 ± 0.16	12.7 ± 1.8	0.46 ± 0.12	0.05 ± 0.02	0.16 ± 0.06
LC	9	8:30	4.7 ± 1.6	0.20 ± 0.13	0.8 ± 0.3	1.9 ± 0.8	0.14 ± 0.05	1.5 ± 0.4	0.05 ± 0.03	0.02 ± 0.01	0.09 ± 0.08
	WS[c] (m/s)	Temp[c] (°C)	RH[c] (%)	Composition (%)							
				Cl^-	NO_3^-	SO_4^{2-}	Na^+	NH_4^+	K^+	Mg^{2+}	Ca^{2+}
HC	1.35 ± 0.49	9.3 ± 6.5	70.6 ± 7.7	2.3 ± 0.8	39.2 ± 7.3	33.2 ± 7.5	0.5 ± 0.3	23.5 ± 1.4	0.9 ± 0.2	0.1 ± 0.0	0.3 ± 0.1
LC	3.09 ± 1.00	14.9 ± 6.5	71.7 ± 14.0	4.5 ± 2.8	17.1 ± 3.7	39.8 ± 4.8	3.4 ± 1.4	31.8 ± 2.6	1.0 ± 0.3	0.5 ± 0.3	1.9 ± 1.2

[a] Mean ± standard deviation are shown for ion concentrations, compositions, and meteorological parameters

[b] Peak time of the sum of ion concentrations

[c] *WS* wind speed, *Temp* temperature, *RH* relative humidity

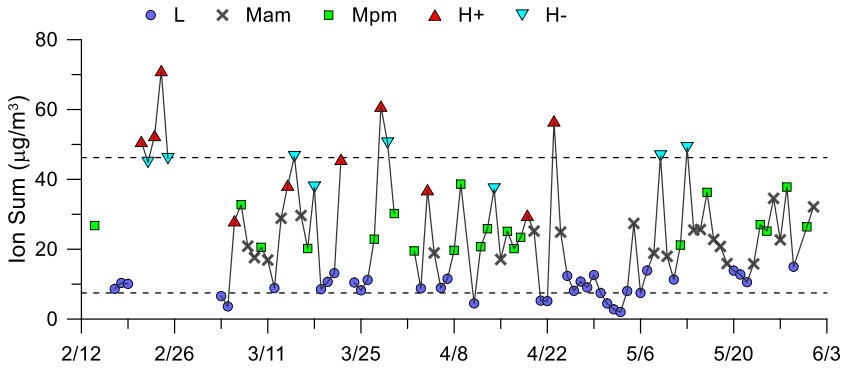

Fig. 5 Occurrences of the diurnal patterns during the first period

temperatures, and high RHs, all of which are favorable for partitioning NO_3^- into the particulate phase.

Figure 6 shows the results from the backward trajectory analysis of H+, H-, and L, in comparison with those between HC and LC days. Isentropic trajectories were calculated using the National Oceanic and Atmospheric Administration (NOAA) Hybrid Single Particle Lagrangian Integrated Trajectory (HYSPLIT) 4 model (Draxler et al., 2012). The meteorological data used for model calculation were from the Global Data Assimilation System of the National Center for Environmental Prediction. The trajectories of air parcels released at the altitude of 500 m at 0900 a.m. local time (0000 UTC) were traced back for 72 h.

The trajectory distances were generally longer for L because wind speeds were higher than those for HC, H+, and H-. The shorter distances of the trajectories of H+ and H-, as well as HC, indicate that the high concentrations of inorganic ions, notably NO_3^-, occurred locally under stagnant conditions (Brook et al., 2002). However, the distance of the trajectory on March 15 was longer despite being classified as HC and H- due to the high wind speed aloft in comparison with low wind speed at the surface (daily mean of 0.9 m/s). Although the concentrations on LC days were lowered further than those of L, their trajectory distances were not particularly longer in comparison. However, it can be seen that many of the trajectories of LC were from, or passed through, the cleaner sectors between the east and south, while a considerable number of the trajectories of L were from the polluted western sector.

Diurnal patterns for other periods

In this section, the diurnal variations for the second and third periods were classified into the patterns distinguished for the first period. The results were then compared with the variations observed in the first period, as shown in Fig. 7. The statistics of selected ions and meteorological parameters for the second and third periods are provided in Table 4. Although

Table 3 Statistical summary of the diurnal patterns[a]

	Number of days	Peak time[b]	Concentration (μg/m³)								
			Sum	Cl^-	NO_3^-	SO_4^{2-}	Na^+	NH_4^+	K^+	Mg^{2+}	Ca^{2+}
H-	8	10:00	44.8 ± 4.5	1.22 ± 0.44	18.7 ± 3.2	13.4 ± 3.6	0.25 ± 0.13	10.7 ± 0.9	0.41 ± 0.12	0.05 ± 0.01	0.16 ± 0.04
H+	10	22:00	47.1 ± 13.2	1.37 ± 0.43	18.4 ± 4.9	15.3 ± 6.6	0.40 ± 0.24	10.9 ± 3.3	0.49 ± 0.13	0.07 ± 0.03	0.20 ± 0.10
Mpm	20	15:30	26.1 ± 6.0	0.87 ± 0.37	9.3 ± 2.1	8.8 ± 3.9	0.28 ± 0.13	6.3 ± 1.7	0.28 ± 0.12	0.05 ± 0.03	0.20 ± 0.12
Mam	21	10:00	22.9 ± 5.4	0.73 ± 0.40	8.0 ± 2.4	7.7 ± 2.4	0.23 ± 0.09	5.7 ± 1.5	0.30 ± 0.11	0.07 ± 0.03	0.19 ± 0.08
L	35	9:30	9.1 ± 3.2	0.41 ± 0.23	2.4 ± 1.3	3.4 ± 1.3	0.20 ± 0.07	2.2 ± 0.8	0.15 ± 0.08	0.06 ± 0.05	0.17 ± 0.13
	WS[c] (m/s)	Temp[c] (°C)	RH[c] (%)	Composition (%)							
				Cl^-	NO_3^-	SO_4^{2-}	Na^+	NH_4^+	K^+	Mg^{2+}	Ca^{2+}
H-	1.69 ± 0.53	9.2 ± 6.3	67.9 ± 7.6	2.8 ± 1.1	41.8 ± 5.9	29.6 ± 6.4	0.6 ± 0.3	23.9 ± 1.4	0.9 ± 0.2	0.1 ± 0.0	0.4 ± 0.1
H+	1.81 ± 0.88	6.7 ± 4.8	73.3 ± 11.0	3.1 ± 1.0	39.7 ± 6.5	31.4 ± 7.1	1.0 ± 0.7	23.1 ± 1.6	1.1 ± 0.5	0.2 ± 0.1	0.5 ± 0.3
Mpm	1.68 ± 0.35	11.8 ± 5.6	68.3 ± 9.3	3.6 ± 2.0	36.4 ± 8.2	32.6 ± 8.9	1.1 ± 0.6	24.1 ± 2.1	1.1 ± 0.4	0.2 ± 0.2	0.8 ± 0.6
Mam	1.83 ± 0.76	13.8 ± 7.1	63.7 ± 9.8	3.3 ± 1.7	35.1 ± 5.8	33.5 ± 6.0	1.0 ± 0.4	24.6 ± 2.1	1.3 ± 0.5	0.3 ± 0.2	0.9 ± 0.4
L	2.51 ± 1.04	11.1 ± 8.7	59.0 ± 12.9	4.6 ± 2.2	25.4 ± 8.1	38.3 ± 6.4	2.5 ± 1.1	25.1 ± 5.1	1.6 ± 0.6	0.7 ± 0.4	1.9 ± 1.2

[a] Mean ± standard deviation are shown for ion concentrations, compositions, and meteorological parameters

[b] Peak time of the sum of ion concentrations

[c] *WS* wind speed, *Temp* temperature, *RH* relative humidity

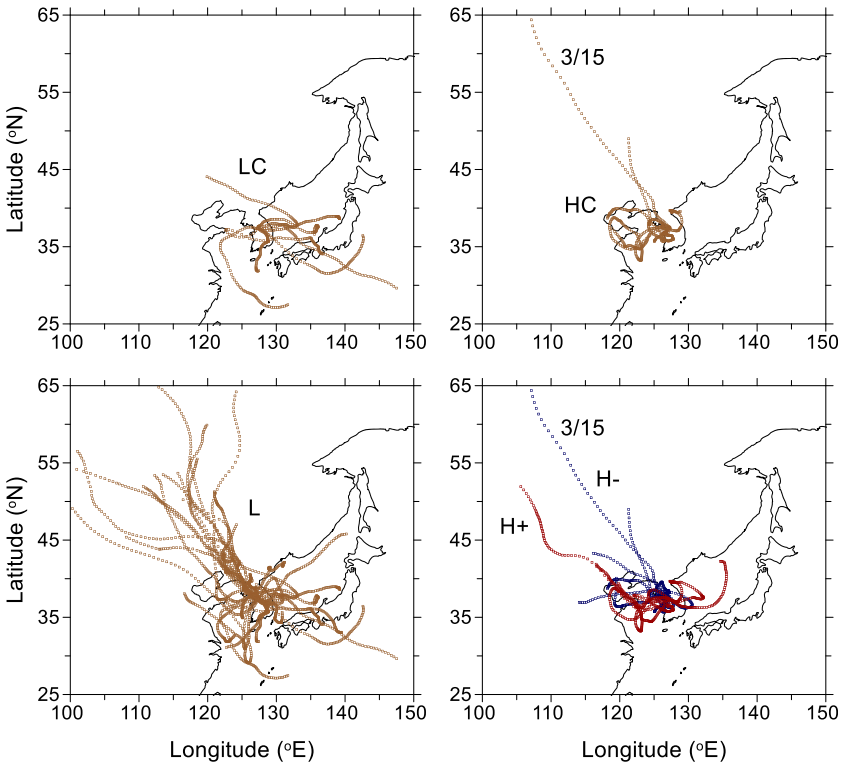

Fig. 6 Three-day backward trajectories for H+, H-, and L for comparison with those on HC and LC days

the characteristic features of the patterns were generally maintained, the differences in the concentration levels among periods were larger for L, Mam, and H+. Figure 7 illustrates that the differences for L and H+ were mainly due to higher concentrations of the third period, as seen in Table 1, while the sum of the third period was the lowest for Mam (Tables 3 and 4).

In the previous section, it was pointed out that the peak was delayed from L to H- with increase of the concentrations of the sum and NO_3^-. In the case of the second period, the variations in the sum and NO_3^- were quite similar to those of the first period. However, increase in the fraction of NO_3^- was not consistent, and the delay of the peak time was not as clear as that for the first period. This is attributable to the fact that photochemical production of secondary ions was not so active due to lower temperatures. Earlier occurrence of the peaks around the noon for Mpm and H+, whose peaks occurred in the afternoon for the first period, was also interpreted as

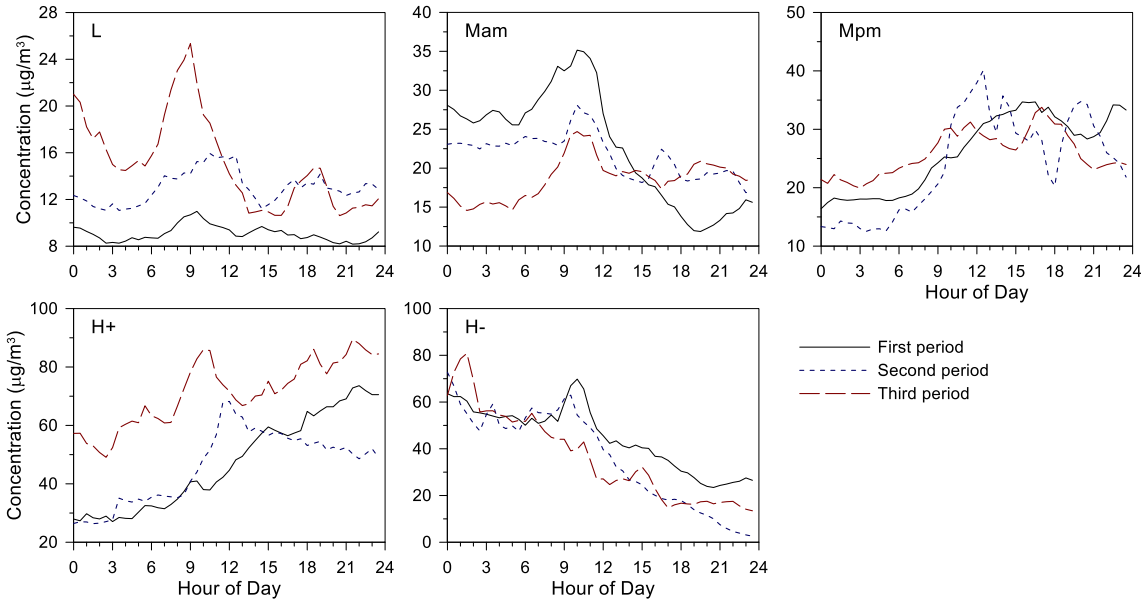

Fig. 7 Comparison of the sums of ion concentrations of the diurnal patterns for the second and third periods with those of the first period

Table 4 Comparison of means of selected variables for the second and third periods

	Second period						Third period					
	Number of days	Peak time[a]	Concentration (μg/m^3)				Number of days	Peak Time[a]	Concentration (μg/m^3)			
			Sum	NO_3^-	SO_4^{2-}	NH_4^+			Sum	NO_3^-	SO_4^{2-}	NH_4^+
H-	2	0:00	36.3	17.3	8.9	8.5	3	1:30	36.6	13.8	12.1	8.5
H+	8	12:00	47.0	15.1	17.3	11.8	8	21:30	71.3	26.7	23.7	17.5
Mpm	3	12:30	24.1	7.6	8.7	6.2	12	17:00	25.8	8.0	9.6	6.6
Mam	10	10:00	21.7	8.2	6.6	5.7	13	10:00	18.7	6.0	6.4	4.9
L	14	10:30	13.0	4.7	4.4	2.8	7	9:00	15.2	3.8	6.4	4.1
	WS[b] (m/s)	Temp[b] (°C)	RH[b] (%)	Composition (%)			WS[b] (m/s)	Temp[b] (°C)	RH[b] (%)	Composition (%)		
				NO_3^-	SO_4^{2-}	NH_4^+				NO_3^-	SO_4^{2-}	NH_4^+
H-	1.53	1.1	82.3	47.6	23.6	23.6	2.86	2.9	62.3	34.9	34.8	22.9
H+	1.12	−0.8	74.5	33.0	36.1	24.7	1.45	10.2	72.5	37.3	32.6	24.5
Mpm	1.44	0.9	86.8	30.6	36.6	26.4	1.61	8.5	65.0	30.9	36.5	25.7
Mam	1.72	−1.7	70.5	35.4	32.4	25.0	1.85	9.4	64.6	31.6	34.9	25.6
L	1.48	−0.2	66.9	36.3	33.5	21.0	2.33	12.2	63.7	23.9	42.8	27.3

[a] Peak time of the sum of ion concentrations

[b] *WS* wind speed, *Temp* temperature, *RH* relative humidity

indicating that the effect of photochemical production was not strong enough to offset the increase in mixing height. Nevertheless, the effects of secondary formation with increasing temperature from L to H- can be seen when grouping the five patterns into three, such as groups of L and Mam, Mpm and H+, and H-, with the delay of the peak times occurring in that order. Note that the sum increased with temperature due to the production of secondary ions. This is different from Table 3, where the sum increased because of preferential partitioning of semi-volatile secondary ions into the particulate phase with decreasing temperature.

The variations for the third period seem to be more similar to those of the first period in Table 3 than those of the second period on the whole. First of all, the peaks were steadily retarded from L to H-. The concentrations of the sum and NO_3^- decreased at H- after an increase to H+, but this was due in part to the high concentrations measured during the third period. In fact, the sum and other concentrations of H+ for the third period, shown in Table 4, were the highest among all the periods (Tables 3 and 4) and on HC days (Table 2). On the other hand, the sum of H- showed a peak just after midnight, which decreased along with higher wind speed and lower RH. Except a few cases, the variations in meteorological parameters for the third period generally coincided well with variations in the sum as well as the concentration and fraction of NO_3^-.

Summary and conclusions

The inorganic ions in $PM_{2.5}$ were measured at a site (127.27°E, 37.34°N, 167 m asl) downwind of Seoul using PILS coupled with IC during three periods. Diurnal patterns were distinguished through a hierarchical cluster analysis during the first period (February to June 2012). The other two periods (November 2012 to January 2013 and March to June 2013) were considered to assess the generality of the patterns identified for the first period. The sum of ion concentrations from the PILS sampling was around 83 % of that determined by filter sampling. Although the slopes of the best fit line and R^2 values were lower for ions with lower concentrations, they fell within reasonable ranges on the whole because each ion concentration was well above its detection limit.

On HC days during the first period, the peak of the sum occurred one hour later in the morning than LC days; the wind speed and temperature for the former were lower than those for the latter. The fraction of NO_3^- was the highest on HC days, while that of SO_4^{2-} was the highest on LC days. The differences between HC and LC days were reproduced more precisely in the five diurnal patterns distinguished for the first period. The peak of the sum occurred during the morning rush hour for L, and was delayed until the next morning for H- with decreasing wind speed and temperature and increasing RH. This suggests that more secondary ions were produced from pollutants accumulated under lower wind speeds, causing a delay in the peak concentration due to the time required to form secondary ions, which overwhelmed the effect of variation in mixing height.

The characteristic features of the patterns in the first period were generally maintained in the patterns of the other two periods, despite some variations in the peak times and concentration levels. This was particularly true for the third period, whose calendar months (March to July) mostly overlapped

with those of the first period (February to June). However, during the second period, which was comprised of colder months, changes in the diurnal patterns from L to H- occurred with increasing temperature, as the effect of increased photochemical formation of NO_3^- was larger than that of increased volatilization in a colder environment.

This study corroborates the basic understanding that high-concentration episodes occur under stagnant conditions. The scientific significance of this study is that detailed variations in secondary formation derived from NO_3^- during increasing the sum of inorganic ion concentrations were demonstrated by analyzing the characteristics of the diurnal patterns. These results can be utilized to devise policy measures to mitigate high concentrations of $PM_{2.5}$ by reducing the secondary formation of inorganic ions and to verify theoretical approaches for the secondary formation of inorganic ions, which is difficult to examine closely due to lack of experimental data.

Acknowledgments This study was supported by the National Research Foundation of Korea (NRF) grant funded by the Korea government (MEST) (no. 2010–0012920), the Korea Meteorological Administration Research and Development Program under the grant KMIPA 2015–6010, and the $PM_{2.5}$ Research Center supported by Ministry of Science, ICT, and Future Planning (MSIP) and the National Research Foundation (NRF) of Korea (NRF-2014M3C8A5030623).

References

Allan MA (2004) Manual for the GAW precipitation chemistry programme: guidelines, data quality objectives and standard operating procedures. No. WMO-TD-1251. World Meteorological Organization, Geneva, Switzerland

Brook JR, Lillyman CD, Shepherd MF, Mamedov A (2002) Regional transport and urban contributions to fine particle concentrations in southeastern Canada. J Air Waste Manage Assoc 52:855–866

Choi SH, Ghim YS, Chang YS, Jung K (2014) Behavior of particulate matter during high concentration episodes in Seoul. Environ Sci Pollut Res 21:5972–5982

Chow JC (1995) Measurement methods to determine compliance with ambient air quality standards for suspended particles. J Air Waste Manage Assoc 45:320–382

Chow JC, Doraiswamy P, Watson JG, Chen LWA, Ho SSH, Sodeman DA (2008) Advances in integrated and continuous measurements for particle mass and chemical composition. J Air Waste Manage Assoc 58:141–163

Draxler R, Stunder B, Rolph G, Stein A, Taylor A (2012) HYSPLIT4 user's guide. http://www.arl.noaa.gov/documents/reports/hysplit_user_guide.pdf. Accessed September 2012

Edgerton ES, Hartsell BE, Saylor RD, Jansen JJ, Hansen DA, Hidy GM (2006) The Southeastern Aerosol Research and Characterization Study, part 3: continuous measurements of fine particulate matter mass and composition. J Air Waste Manage Assoc 56:1325–1341

Fine PM, Jaques PA, Hering SV, Sioutas C (2003) Performance evaluation and use of a continuous monitor for measuring size-fractionated $PM_{2.5}$ nitrate. Aerosol Sci Technol 37:342–354

Fine PM, Sioutas C, Solomon PA (2008) Secondary particulate matter in the United States: insights from the particulate matter supersites program and related studies. J Air Waste Manage Assoc 58:234–253

Fujita EM, Stockwell WR, Campbell DE, Keislar RE, Lawson DR (2003) Evolution of the magnitude and spatial extent of the weekend ozone effect in California's South Coast Air Basin, 1981–2000. J Air Waste Manage Assoc 53:802–815

Ghim YS, Chang YS, Jung K (2015) Temporal and spatial variations in fine and coarse particles in Seoul, Korea. Aerosol Air Qual Res 15: 842–852

IPCC (2013) Climate change 2013. In: Stocker TF, Qin D, Plattner G-K, Tignor MS, Allen K, Boschung J, Nauels A, Xia Y, Bex V, Midgley PM (eds) The Physical Science Basis. Contribution of Working Group I to the Fifth Assessment Report of the Intergovernmental Panel on Climate Change. Cambridge University Press, Cambridge, UK and New York, NY, USA

Kim CH, Choi Y, Ghim YS (2015) Characterization of volatilization of filter-sampled $PM_{2.5}$ semi-volatile inorganic ions using a backup filter and denuders. Aerosol Air Qual Res 15:814–820

Khlystov A, Wyers G, Slanina J (1995) The steam-jet aerosol collector. Atmos Environ 29:2229–2234

Lee T (2002) The ionic composition of aerosol in Big Bend National Park. Colorado State University, M. S. thesis, Colorado

Lee T, Yu XY, Kreidenweis SM, Malm WC, Collett JL (2008) Semi-continuous measurement of $PM_{2.5}$ ionic composition at several rural locations in the United States. Atmos Environ 42:6655–6669

Makkonen U, Virkkula A, Mäntykenttä J, Hakola H, Keronen P, Vakkari V, Aalto PP (2012) Semi-continuous gas and inorganic aerosol measurements at a Finnish urban site: comparisons with filters, nitrogen in aerosol and gas phases, and aerosol acidity. Atmos Chem Phys 12:5617–5631

Malm WC, Day DE, Carrico C, Kreidenweis SM, Collett JL, McMeeking G, Lee T, Carrillo J, Schichtel B (2005) Intercomparison and closure calculations using measurements of aerosol species and optical properties during the Yosemite Aerosol Characterization Study. J Geophys Res 110:D14302. doi:10.1029/2004JD005494

Maxwell-Meier K, Weber R, Song C, Orsini D, Ma Y, Carmichael GR, Streets DG (2004) Inorganic composition of fine particles in mixed mineral dust–pollution plumes observed from airborne measurements during ACE-Asia. J Geophys Res 109:D19S07. doi:10.1029/2003JD004464

Millstein DE, Harley RA, Hering SV (2008) Weekly cycles in fine particulate nitrate. Atmos Environ 42:632–641

Orsini DA, Ma Y, Sullivan A, Sierau B, Baumann K, Weber RJ (2003) Refinements to the particle-into-liquid sampler (PILS) for ground and airborne measurements of water soluble aerosol composition. Atmos Environ 37:1243–1259

Pancras JP, Landis MS, Norris GA, Vedantham R, Dvonch JT (2013) Source apportionment of ambient fine particulate matter in Dearborn, Michigan, using hourly resolved PM chemical composition data. Sci Total Environ 448:2–13

Ryu SY, Kim JE, Zhuanshi H, Kim YJ, Kang GU (2004) Chemical composition of post-harvest biomass burning aerosols in Gwangju, Korea. J Air Waste Manage Assoc 54:1124–1137

Ryu SY, Kwon BG, Kim YJ, Kim HH, Chun KJ (2007) Characteristics of biomass burning aerosol and its impact on regional air quality in the summer of 2003 at Gwangju, Korea. Atmos Res 84:362–373

Seinfeld JH, Pandis SN (1998) Atmospheric chemistry and physics: from air pollution to climate change. John Wiley & Sons, New York, NY, Chapter 9

Seoul Institute (2010) Characterization of fine particles through intensive field monitoring in Seoul. Seoul, Korea (in Korean)

Simon PK, Dasgupta PK (1995) Continuous automated measurement of the soluble fraction of atmospheric particulate matter. Anal Chem 67:71–78

Solomon PA, Sioutas C (2008) Continuous and semicontinuous monitoring techniques for particulate matter mass and chemical components: a synthesis of findings from EPA's particulate matter

supersites program and related studies. J Air Waste Manage Assoc 58:164–195

Solomon PA, Hopke PK, Froines J, Scheffe R (2008) Key scientific findings and policy-and health-relevant insights from the US Environmental Protection Agency's Particulate Matter Supersites Program and related studies: an integration and synthesis of results. J Air Waste Manage Assoc 58(13 Suppl):S3–S92

Sorooshian A, Brechtel FJ, Ma Y, Weber RJ, Corless A, Flagan RC, Seinfeld JH (2006) Modeling and characterization of a particle-into-liquid sampler (PILS). Aerosol Sci Technol 40:396–409

Stolzenburg MR, Hering SV (2000) Method for the automated measurement of fine particle nitrate in the atmosphere. Environ Sci Technol 34:907–914

Thompson JE, Hayes PL, Jimenez JL, Adachi K, Zhang X, Liu J, Weber RJ, Buseck PR (2012) Aerosol optical properties at Pasadena, CA during CalNex 2010. Atmos Environ 55:190–200

Watson JG (2002) Visibility: science and regulation. J Air Waste Manage Assoc 52:628–713

Weber R, Orsini D, Duan Y, Baumann K, Kiang CS, Chameides W, Lee YN, Brechtel F, Klotz P, Jongejan P, Ten Brink H, Slanina J, Boring CB, Genfa Z, Dasgupta P, Hering S, Stolzenburg M, Dutcher DD, Edgerton E, Hartsell B, Solomon P, Tanner R (2003) Intercomparison of near real time monitors of PM2.5 nitrate and sulfate at the U.S. Environmental Protection Agency Atlanta Supersite. J Geophys Res 108:8421. doi:10.1029/2001JD001220

Weber RJ, Orsini D, Daun Y, Lee YN, Klotz PJ, Brechtel F (2001) A particle-into-liquid collector for rapid measurement of aerosol bulk chemical composition. Aerosol Sci Technol 35:718–727

WHO (World Health Organization) (2006) Health risks of particulate matter from long-range transboundary air pollution. WHO regional office for Europe. Copenhagen, Denmark

Wittig AE, Takahama S, Khlystov AY, Pandis SN, Hering S, Kirby B, Davidson C (2004) Semi-continuous $PM_{2.5}$ inorganic composition measurements during the Pittsburgh Air Quality Study. Atmos Environ 38:3201–3213

Won SR, Choi Y, Kim AR, Choi SH, Ghim YS (2010) Ion concentrations of particulate matter in Yongin in spring and fall. J Korean Soc Atmos Environ 26:265–275 (in Korean with English Abstract)